Optimal design and operation of dual-ejector PEMFC hydrogen supply and circulation system

Chen, L., Xu, K., Yang, Z., Yan, Z., & Dong, Z.

2022

energies

MDPI

Article

Optimal Design and Operation of Dual-Ejector PEMFC Hydrogen Supply and Circulation System

Li Chen [1,2,*], Keda Xu [1], Zuyong Yang [2], Zhen Yan [2] and Zuomin Dong [1,*]

[1] Department of Mechanical Engineering, Institute for Integrated Energy Systems, University of Victoria, Victoria, BC V8W 2Y2, Canada; kedaxu@uvic.ca
[2] Beijing Yijiajiequ Tech Inc., Beijing 100081, China; zuyong.yang@cncapsit.cn (Z.Y.); zhen.yan@cncapsit.cn (Z.Y.)
* Correspondence: chenli@uvic.ca (L.C.); zdong@uvic.ca (Z.D.)

Abstract: A proton exchange membrane fuel cell (PEMFC) system requires an adequate hydrogen supply and circulation to achieve its expected performance and operating life. An ejector-based hydrogen circulation system can reduce the operating and maintenance costs, noise, and parasitic power consumption by eliminating the recirculation pump. However, the ejector's hydrogen entrainment capability, restricted by its geometric parameters and flow control variability, can only operate properly within a relatively narrow range of fuel cell output power. This research introduced the optimal design and operation control methods of a dual-ejector hydrogen supply/circulation system to support the full range of PEMFC system operations. The technique was demonstrated on a 70 kW PEMFC stack with an effective hydrogen entrainment ratio covering 8% to 100% of its output power. The optimal geometry design ensured each ejector covered a specific output power range with maximized entrainment capability. Furthermore, the optimal control of hydrogen flow and the two ejectors' opening and closing times minimized the anode gas pressure fluctuation and reduced the potential harm to the PEMFC's operation life. The optimizations were based on dedicated computational fluid dynamics (CFD) and system dynamics models and simulations. Bench tests of the resulting ejector-based hydrogen supply/circulation system verified the simulation and optimization results.

Keywords: hydrogen ejectors; dual-ejector system; PEM fuel cell; hydrogen supply and circulation; CFD simulation; optimal design; optimal control

Citation: Chen, L.; Xu, K.; Yang, Z.; Yan, Z.; Dong, Z. Optimal Design and Operation of Dual-Ejector PEMFC Hydrogen Supply and Circulation System. *Energies* **2022**, *15*, 5427. https://doi.org/10.3390/en15155427

Academic Editors: Pierpaolo Polverino and Cesare Pianese

Received: 27 June 2022
Accepted: 25 July 2022
Published: 27 July 2022

1. Introduction

Proton exchange membrane fuel cells (PEMFCs) rely on the accurate control and continuous supply of hydrogen fuel (H_2) and oxidant air (O_2) to produce electricity with byproducts of heat and water. PEMFC and green hydrogen from renewable energies present a promising technological solution to substitute for internal combustion engines (ICEs) as a highly efficient, zero-emission energy converter. The combination can address the issues of air pollution, global warming, and fluctuating petroleum fuel supply for transportation and power generation.

The anode H_2 supply and circulation system of a PEMFC provides excessive fuel and recycles the unused hydrogen from the fuel cell stack back to the hydrogen supply stream to help maintain the ideal temperature, humidity, and quality of the hydrogen fuel. The compressed H_2 in storage tanks must be regulated to the targeted pressure (usually 1.5 MPa) and the required H_2 mass flow rate using pressure regulators, proportional valves, or injector(s) [1]. A mechanical pump is traditionally used to recirculate the unconsumed hydrogen, as in the PEMFC system of the world's first mass-produced fuel cell vehicle (FCV), the Toyota Mirai [2]. Although reliable, mechanical pumps or blowers may corrode over time, and pump lubricant is a potential source of membrane poisoning, in addition

to the parasitic power consumption by the pump. An ejector, if properly designed, can perform the circulation task with a reduced parasitic power consumption for the PEMFC system, as well as system weight and volume. Multiple ejectors can effectively circulate the unconsumed hydrogen over a broader range of the PEMFC system's power output. Ejectors have been widely applied in many industries, such as air conditioning and refrigeration systems, to replace mechanical compressors since their introduction in the early 1900s [3]. A typical ejector adopts a Venturi nozzle to create a high-speed stream with low pressure to suck another stream and reinject it to the main stream [4]. H_2 ejectors used in the PEMFC system take advantage of the considerable H_2 pressure potential energy between the fuel tank and the stack (i.e., the primary flow) to create a pressure drop through a nozzle to suck the unused gas (i.e., the secondary flow) with no power consumption. However, the ejector's hydrogen entrainment capability is restricted by its geometry, gas flow rate, and pressure drop. Due to the system's advantages of a simple structure, no moving components, and zero energy consumption, other automotive manufacturers, such as Honda [5,6] and Hyundai [7], have adopted ejectors in the PEMFC system of their FCVs.

Gas ejector design is challenging, especially for a PEMFC system, due to the broad range of a PEMFC's power output and the resulting wide variation in the hydrogen flow rate. Many researchers have studied the ejector's hydrogen entrainment ratio using numerical analysis [8,9]. A significant issue of the ejector with fixed geometries is that the ejector's pressure is limited due to PEMFC stack anode system conditions. As a result, the hydrogen entrainment ratio of the ejector falls rapidly when the primary gas flow rate deviates from the design points, resulting in a narrow operating power range. Three different solutions have been suggested to address this problem [9]: (i) variable-flow ejectors with a changeable nozzle diameter, (ii) multi-ejectors with more than one constant ejector, and (iii) a combination of an ejector and a pump. The ejectors proposed in [10,11], which used a needle inside the small nozzle opening to change its size, can provide a considerable range of primary mass flow rate and improve overall entrainment performance. To accurately control the needle position, diaphragms [11] and electronically controlled motors [10] were applied and tested. The diaphragms' positions were adjusted by the pressure difference between the oxidizing gas and supplied fuel. The movement of the needle attached to the diaphragms was then changed during different operating conditions [11]. A stepper motor can also perform this task by precisely controlling the needle's displacement.

However, the needle sealing at elevated pressures and the central alignment of the actuator shaft are major concerns for the variable flow ejector, provoking significant challenges for real-life and long-duration applications. Two or more ejectors working in parallel were also proposed to better suit the rapid change operations of fuel cell vehicles. Compared to a single ejector, multi-ejector performance is better in the overall operating range. However, previous studies that employed a double ejector for a PEMFC simply multiplied the results of the single ejector by two [12], and the proposed multi-ejectors did not show an excellent performance improvement without a systematical design and optimal control. Using the combination of an ejector and a pump for a PEMFC stack fuel-delivery system was also proposed [13]. However, taking advantage of these two devices also will result in encountering drawbacks and increasing control difficulties and design complexities.

So far, no reported work has demonstrated the ability to support the full-power operation range of large PEMFC stacks using only ejectors. Even with variable ejectors proposed in previous studies, their performance and coverage are still minimal. The authors of [8] compared three different ejector solutions for a 12.5 kW PEMFC stack used in a forklift system: (i) a single ejector covering the operating range of about 85–180 A (or 6.7–12.5 kW), (ii) dual ejectors covering 60–180 A (or 4.9–12.5 kW), and (iii) a variable nozzle geometry solution also covering 60–180 A. These solutions could not fully cover the full range of the PEMFC stack operation between 15 and 180 A. In [9], the researchers designed an ejector with fixed geometries for a 5 kW stationary PEMFC system and compared it with different simulation models. A variable multi-ejector consisting of two constant nozzle ejectors and one solenoid valve was proposed in [12] for a minibus PEMFC system, demonstrating

a practical entrainment ratio lower than one for the operation range. An electronically controlled variable flow ejector using needles in the nozzle throat could perform the gas recirculation for a Ballard Mark 9 stack between 7 and 17 kW [10]. Ejectors were also adopted in the H_2/O_2 PEMFC stack; e.g., using a dual-ejector system with one ejector to recirculate H_2 and one to recirculate O_2. They showed potential benefits for water management and performance improvement in closed-space or environment applications such as crewless underwater vehicles and spacecraft [14].

This paper focused on the optimal design and operation control of two ejectors for H_2 supply/circulation over the entire operating range of a PEMFC system, covering the stack's minimum 8% to maximum 100% power output. The design could effectively support full-range PEMFC system operation, given that the PEMFC system's parasitic power consumption was about 8–15%.

This work did not use ejectors with a changeable nozzle geometry [10,15] to avoid their control complexity, reliability issues, and high manufacturing cost. Instead, it used two ejectors with different nozzle dimensions to cover different PEMFC power output sections in the full range. The design optimization best distributed these ranges with no gaps and useless overlaps. On the other hand, the optimal operation control ensured smooth transitions between these two ejectors when the power output of the PEMFC system dramatically increased or decreased. These ejectors with optimally designed geometries, in cooperation with electronically controlled mass flow rate regulators, adjusted the primary flow to achieve a high hydrogen entrainment ratio and a wide operation range.

Specifically, this study modeled, simulated, designed, and tested a dual-ejector system for a PEMFC stack with maximum output power (P_{max}) of 70 kW. With the optimal control of the dual-ejector system, it could satisfy the stack operation conditions from the idle 6 kW to the maximum 70 kW power, ranging from 8% to 100% of P_{max}. The H_2 supply and circulation system using dual ejectors for the PEMFC stack are presented in Section 2. The optimal design of each ejector's geometrical parameters are introduced in Section 3, based on the computational fluid dynamics (CFD) simulation and analysis, the test results for each ejector, and the comparisons to the CFD results. Section 4 presents the optimal control and test of the dual-ejector system, which could fulfill the required stack H_2 stoichiometric ratio during the entire operating range. The anode gas pressure fluctuation was also studied and analyzed when shifting between different ejectors during operation. Conclusions regarding key findings are presented in Section 5.

2. Anode Hydrogen Supply System Design with Two Ejectors

The PEMFC stack of the targeted anode hydrogen supply and recirculation system had a maximum output power of 70 kW. The stack operation current was from 40 A to 600 A, corresponding to a total stack voltage ranging from 158 V to 115 V, providing 6 kW of idle power and 70 kW of maximum power. The anode inlet and outlet pressure, mass flow rate, temperature, and required hydrogen stoichiometric ratio $\omega_{H_2\_SR}$ are critical parameters in anode hydrogen supply and recirculation system design, with some of these parameters plotted in Figure 1. The stoichiometric ratio of H_2 $\omega_{H_2\_SR}$ defines the total requested H_2 delivered to the stack over the theoretical reacted H_2. The unconsumed hydrogen from the stack anode outlet must be recirculated back to the primary stream to facilitate the ideal hydrogen fuel temperature and relative humidity (RH). The hydrogen gas temperature in the primary ejector inlet was assumed to be 293.15 K, and the anode outlet mixture was between 327.15 K and 348.15 K with 100% RH. Therefore, depending on the operation conditions, the required RH of anode inlet gas was between 40% and 80%.

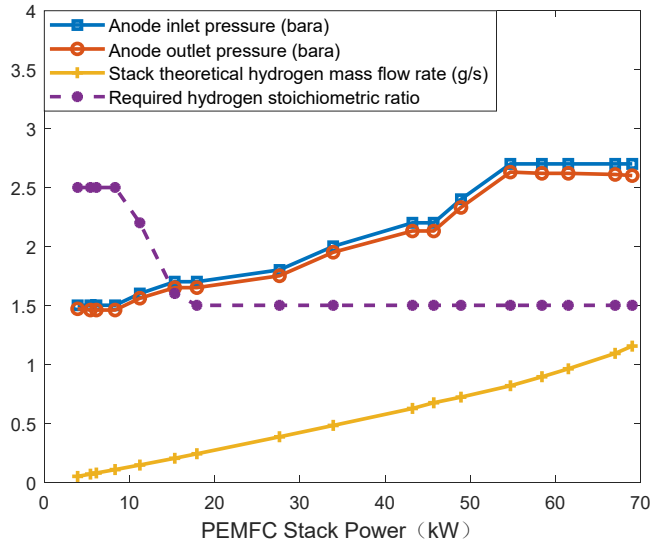

Figure 1. H_2 inlet and outlet pressure, mass flow rate, and stoichiometric ratio.

2.1. Design of Dual-Ejector System

A dual-ejector gas recirculation device was designed to cover a wide range of operations from 40 to 600 A. Ejector A and Ejector B, as shown in Figure 2, each had a unique, optimized geometric parameter to cover a specific range of the PEMFC system's operation. A three-way ball valve was used to switch flows between the two different paths. One or two proportional valves (PVs) could control the dual-ejector's pressure and mass flow rate. One PV could satisfy the functional requirements, but also could induce system pressure fluctuation during the transition process when the three-way valve shifted the hydrogen path from Ejector A to B or backward. Therefore, two PVs, with each PV corresponding to one ejector, were proposed, as shown in Figure 2b. The dynamic pressure response and anode inlet pressure changes between the two ejectors were investigated and tested, the results of which are presented in a later section.

The compressed H_2 from the fuel tank was reduced to 15 bara (absolute pressure) using pressure regulators before entering the mass/pressure control valves. Depending on the PEMFC operation status, the mass/pressure control valve had to adjust the H_2 pressure and mass flow rate and inject high-pressure gas into the ejector to pump the unused gas. Finally, the two flows were mixed and ejected to the PEMFC anode with a low pressure between 1.5 and 2.7 bara based on the stack requirement. During the mixing process in the ejector, the dry primary hydrogen gas flow was humidified by the circulated used-hydrogen gas mixture; therefore, there no humidifier was needed in this system.

This integrated dual-ejector hydrogen supply and recirculation system's optimal design had to rely on the specific PEMFC stack requirements. The main steps included:

(i) Calculating the minimum and maximum fuel mass flow rate and pressure drops for the wide-range operating conditions;
(ii) Choosing the appropriate fuel injector or pressure/mass flow rate regulator;
(iii) Optimal design of each ejector's geometric parameters to enlarge its entrainment capability to fulfill the requested fuel stoichiometric ratio during the minimum and maximum operating conditions;
(iv) Optimal control of the integrated hydrogen supply system using successively or simultaneously working injectors to cover the full range of dynamic fuel cell power changes.

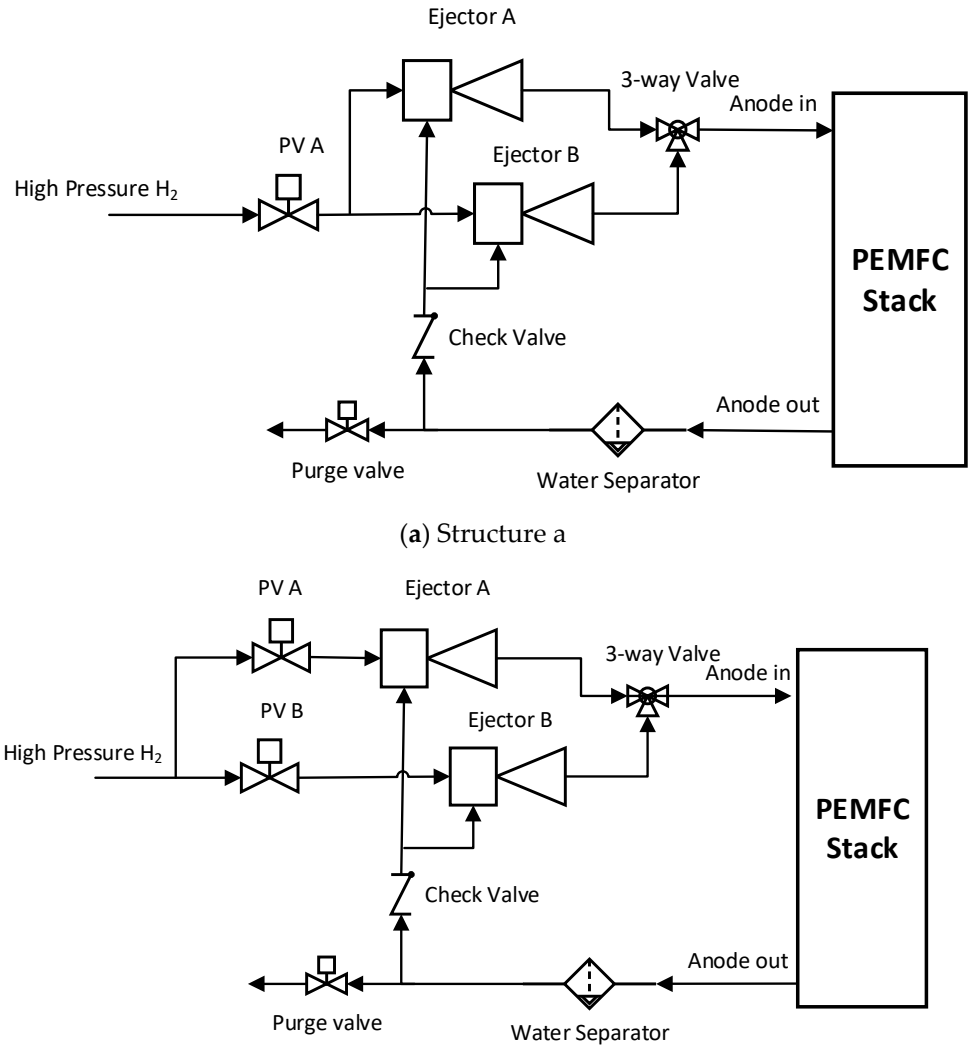

(**a**) Structure a

(**b**) Structure b

Figure 2. Dual-ejector hydrogen supply and recirculation system: (**a**) using one proportional valve (PV A); (**b**) using two proportional valves (PV A and PV B).

To achieve these goals, a CFD simulation of the ejectors and the optimal control methods, as well as the ejector sample tests, validation, and performance analysis, were carried out step by step.

2.2. Hydrogen Gas Pressure and Flow Rate Control

The anode hydrogen gas pressure and mass flow rate control rely on the accurate gas injection from a high-pressure tank. The mainstream of high-pressure H_2 from this injection system usually adopts electronically controlled devices, such as injectors or proportional valves. They are crucial in ensuring fuel mass and pressure supply to the anode side.

Both H_2 injectors and proportional valves rely on the electric current to generate magnetic forces to open and close the valve by lifting the plunger against the spring force and letting the gas flow. Advanced proportional control solenoid valves can precisely change the intensity of the coil current or the magnetic power to influence the valve's opening degree. As a result, the flow rate can be freely controlled in proportion to the control signal. The control signal is usually converted into a pulse-width modulation (PWM) signal to eliminate hysteresis effects to prevent the static friction generated during the plunger's movement. By adjusting the PWM frequency and duty cycle, the variable coil current can control the flow rate precisely in a proportional solenoid valve.

A proportional control solenoid valve was chosen in this study for the H_2 supply system, since it could operate at a higher pressure and sustain a wide range of inlet/outlet pressure differences. The proportional valve's orifice design was essential for the continuous and smooth control of the variable flow rate. The most important parameters for selecting a correct solenoid valve are the flow coefficient (the k_v value in m^3/h or c_v value in gallons/min), the maximum operating pressure range (i.e., the pressure before and after the valve P_{in} and P_{out}), and the requested maximum flow rate. This paper took k_v values measured with the water's flow rate at 293.15 K and 1 bar relative pressure at the valve inlet, compared with 0 bar at the valve outlet. For gases, the standard flow rate Q_N was calculated depending on the low and high flow pressure drops through the valve orifice. The flow characteristics could change if the differential pressure between inlet and outlet pressure exceeded half the inlet pressure value. Specifically, the calculation of the standard flow rate for subcritical conditions; i.e., $P_{out} > 0.5283P_{in}$, is:

$$Q_N = 514k_v\sqrt{\frac{P_{out}(P_{in} - P_{out})}{T_{in}\rho_N}} \tag{1}$$

For critical flow, where $P_{out} < 0.5283P_{in}$, the standard flow rate is determined by:

$$Q_N = 257k_vP_{in}\sqrt{\frac{1}{T_{in}\rho_N}} \tag{2}$$

where Q_N and ρ_N are the standard flow rate and gas density at 0 °C and 1 atm, respectively; k_v is the flow coefficient determined by the proportional valve; T and P are the temperature and pressure, respectively; and subscripts *in* and *out* represent the inlet and outlet of the valve, respectively.

The characteristic curves of a proportional valve with constant inlet pressure of 15 bara are plotted in Figure 3. The hydrogen volume flow rate (Q in NLPM, or normal liter per minute) of different valve lift at temperature 293.15 K versus the pressure differences ($dP = P_{in} - P_{out}$) were adjustable with different k_v values. The k_v value could be controlled by the PWM control signal, where the position of the plunger was determined by the coil current.

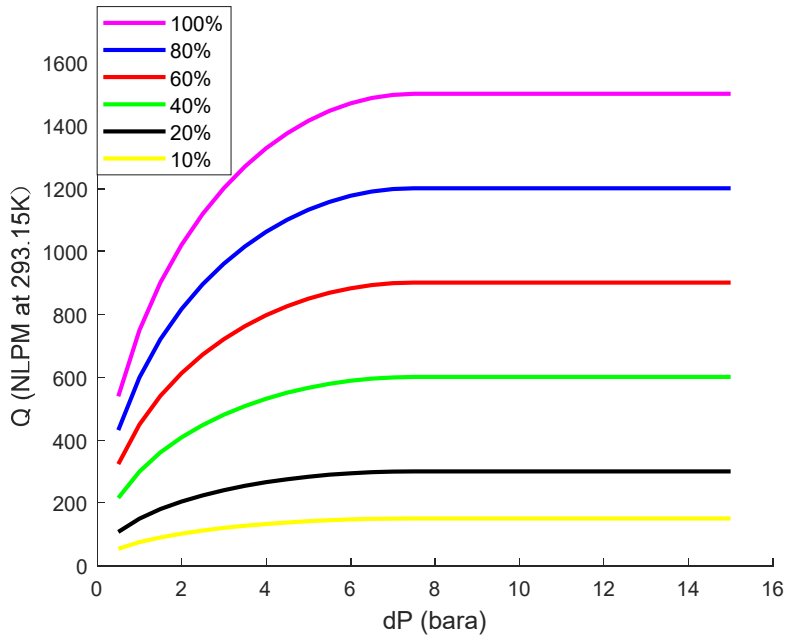

Figure 3. Hydrogen flow rate characteristics of the proportional valve.

The PWM-controlled proportional valve offered a flexible range of pressure outlets at different mass flow rates. In this test, the downstream pressure could range from 14.5 to 1 bara by adjusting the duty cycle and k_v value, allowing the optimal control to achieve a variable flow rate in a wide range of operations.

3. Ejector Design, Simulation, and Test

The optimal design of a hydrogen ejector's geometric parameters is vital to ensure requested gas recirculation during an extensive range of fuel cell operations. First, using CFD simulations, this study modeled and analyzed the primary and secondary gas flows to understand the pressure and velocity changes during the entrainment process. Then, based on the ejector's working principles, key geometry parameters were optimized to achieve a wide range of entrainment ratios for the designed fuel cell stack. After that, ejector samples were created and tested to verify their performance.

3.1. Ejector Working Principles

A gas ejector usually contains four parts: a primary nozzle, a suction chamber, a mixing section, and a diffuser (Figure 4). The primary stream flows through a nozzle inside the suction chamber, entrains the secondary stream, and mixes with the outlet through the mixing section and diffuser. The critical parameter in the ejector design is the diameter of the Venturi nozzle (D_n), which can significantly reduce the local pressure of the primary flow to entrain the secondary flow into the stream without using any power. The Venturi effect can accelerate the gas flow speed through the nozzle by narrowing the gas path. In this work, we assumed that the primary flow pressure P_1 and mass flow rate $\dot{m}_1$ could be controlled and adjusted by the proportional valve, as discussed in the previous section. The outlet pressure and mass flow, P_2 and $\dot{m}_2$, were determined by the PEMFC stack anode inlet requirement. The secondary inlet pressure and mass flow, P_3 and $\dot{m}_3$, were confined by the stack anode outlet conditions. Other key geometry parameters of the ejector are also demonstrated in Figure 4.

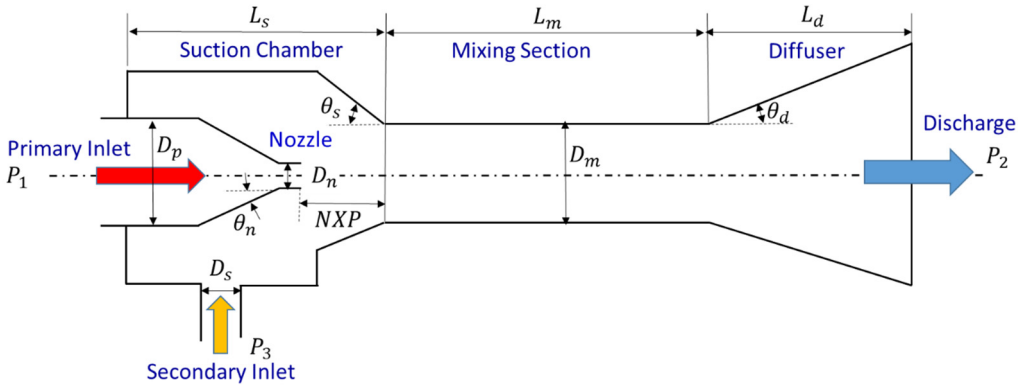

Figure 4. Schematic diagram of an ejector.

According to the principle of mass continuity and the Bernoulli effect, the velocity of an ideal gas must increase when it passes through a constricted area. In fluid dynamics, the principle of conservation of energy states that an increase in fluid speed coincides with a decrease in static pressure. Thus, when the primary hydrogen gas with a static pressure passes through the nozzle inside the ejector, the static pressure of the primary flow at the nozzle outlet will be reduced to a level lower than the pressure of the secondary flow at the suction port.

The operational modes of an ejector can be divided into three regions depending on the back pressure: (i) the double-choking mode (or critical model), in which the ejector's entrainment ratio is kept constant, and both the primary and the secondary stream reach critical mode; (ii) the single-choking mode (or subcritical mode), in which the entrainment ratio is reduced due to the decreasing of secondary flow rate; and (iii) the backflow mode,

in which the entrainment ratio drops to zero, and the ejector fails to operate. The maximum entrainment ratio of ejectors can be reached when both the primary and secondary inlets reach choking conditions; i.e., in the critical mode, they are mainly dependent on the PEMFC's operation conditions. The mass flow rate of primary inlet gas ($\dot{m}_1$) is restricted by the nozzle diameter. Assuming the primary and secondary flows have uniform distributed velocities in the radial direction, a 1D mathematical model can be built to determine some key parameters [16]. For an ideal compressible gas, when the primary flow occurs at the choking condition at the nozzle, the Mach number equals one and the mass flow rate $\dot{m}_1$ is calculated as:

$$\dot{m}_1 = C_d \frac{\pi D_n^2 P_1}{4\sqrt{T_1}} \sqrt{\frac{\gamma}{R_g}\left(\frac{2}{\gamma+1}\right)^{\frac{\gamma+1}{\gamma-1}}} \tag{3}$$

where P_1 and T_1 are the total pressure and temperature of the primary flow, respectively; D_n is the diameter of nozzle throat, γ is the gas-specific heat ratio, R_g is the gas constant, and C_d is the discharge ratio.

The ejector performance was measured using the hydrogen entrainment capability ω_{H_2}. If the required hydrogen stoichiometric ratio $\omega_{H_2\_SR}$ was smaller than the ω_{H_2}, the ejector was considered to be functional.

$$\omega_{H_2} = \frac{\dot{m}_3}{\dot{m}_1} y_{H_2} + 1 \tag{4}$$

where $\dot{m}_3$ is the mass flow rate of entrained flow from secondary inlet and y_{H_2} is the volumetric ratio of hydrogen gas in the entrained secondary flow.

3.2. Ejector Design and CFD Simulations

The CFD simulations were conducted using ANSYS Fluent, and assumed the working fluid was an ideal compressible gas in a steady-state condition. The 3D axisymmetric ejector fluid domain was generated in Siemens NX 12 and imported into the ANSYS Fluent environment for domain meshing and simulation. The SST k-ω model was adopted to solve the coupled momentum balance and pressure-based continuity equations, as suggested in [9]. Boundary conditions of the CFD simulations were set based on the PEMFC stack realistic specifications shown in Figure 1. The primary hydrogen temperature was set at 293.15 K, and the primary inlet was a mass flow rate inlet. The ejector outlet and secondary inlet were set with a constant pressure depending on the operating conditions of the fuel cell stack. The simulation results of the ejector's pressure, velocity, temperature, and H_2 mass fraction in the symmetric plane at the maximum PEMFC operating condition (70 kW) are presented in Figure 5.

The entrainment ratio of an ejector can vary, mainly depending on its critical geometric parameter. The most crucial ejector geometries include the nozzle throat diameter (D_n), the mixing chamber diameter (D_m) and length (L_m), the nozzle exit position (NXP) relative to the mixing section, the diffuser length (L_d), and the nozzle convergence and diffuser divergence angle (θ). The values of NXP, L_m, and L_d depend on the value of D_m that is proportional to the nozzle throat diameter D_n. Since D_n is fixed and determined by the previous equations, the most important thing is to find the optimized value for five unknown variables: $x_1 = \frac{D_m}{D_n}$, $x_2 = \frac{NXP}{D_m}$, $x_3 = \frac{L_m}{D_m}$, $x_4 = \frac{L_d}{D_m}$, and $x_5 = \theta_d$. Each variable has a lower and upper boundary; these have been investigated in many other studies [8,9,17].

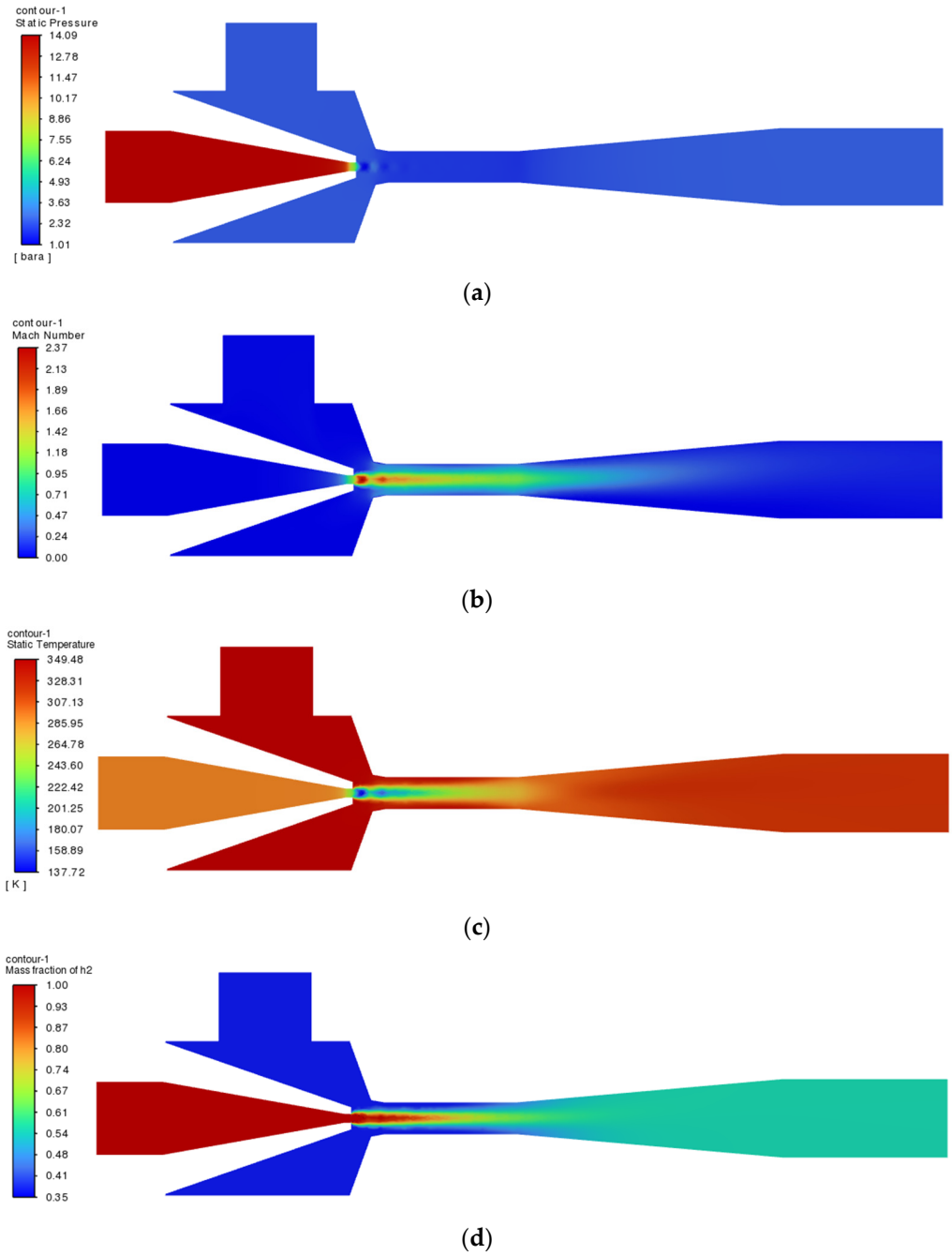

Figure 5. CFD simulation results: (**a**) pressure; (**b**) velocity; (**c**) temperature; (**d**) H_2 mass fraction.

In this study, we wanted to ensure that the hydrogen entrainment capability ω_{H_2} was large enough for a wide range of operating conditions. Based on the PEMFC stack specifications, the ejector boundary conditions varied, according to its power, from 6 to 70 kW. Two ejectors were needed to cover the full range of operation. The maximum nozzle throat diameter for the two ejectors was calculated based on Equations (2) and (3). Each ejector had to provide a sufficient entraining capability in a specific range of power levels. Specifically, the fuel cell stack listed 17 operating points with different hydrogen inlet and outlet pressures and mass flow rates. The optimal design of an ejector must find the best geometric parameters to maximize the hydrogen entrainment capability in

different operating conditions, subject to some constraints. To obtain the optimum variable $x = [x_1, x_2, x_3, x_4, x_5]'$, this problem can be formulated as below:

$$\max_x w = \omega_{H_2,i}, \quad i = 1, \ldots, n subject to: \begin{bmatrix} 3 \\ 0.75 \\ 3 \\ 6 \\ 2 \end{bmatrix} \leq x \leq \begin{bmatrix} 6 \\ 1.13 \\ 5 \\ 20 \\ 10 \end{bmatrix} \tag{5}$$

where $\omega_{H_2,i}$ is the hydrogen entrainment capability at the i^{th} operation point and n is the total number of operation points.

This work used the trial-and-error method to determine the five key parameters. We found that the optimal geometric parameters were very case-dependent, and could hardly adopt optimization algorithms such as artificial neural networks or genetic algorithms [17]. The results (D_m and L_m) during the trial-and-error processes to determine the main geometric parameters of the ejector B are plotted in Figure 6. It can be seen that in the PEMFC's high-load operation conditions (primary flow rate 300–800 NLPM), D_m had a great influence on the ω_{H_2}. As D_m increased, the ω_{H_2} was promoted dramatically, and the optimal D_m was 4.8 mm given the entrainment performance in low load conditions below 300 NLPM. The L_m mildly affected the ω_{H_2} during the high primary flow rate (600–800 NLPM), but a smaller L_m resulted in a higher ω_{H_2} in relatively lower load operation conditions. Hence, for ejector B, the optimal L_m could be either 16 mm or 20 mm, and the ratio L_m / D_m was 3.33, which was close to the result given in [18]. After CFD optimization, Ejector A supported stack operations for the lower power range between 6 and 27 kW (primary inlet pressure 2.8–14.4 bara), while Ejector B did so for the upper power range between 27 and 70 kW (primary inlet pressure 4.6–13.9 bara). The optimized geometric dimensions of Ejectors A and B are listed in Table 1.

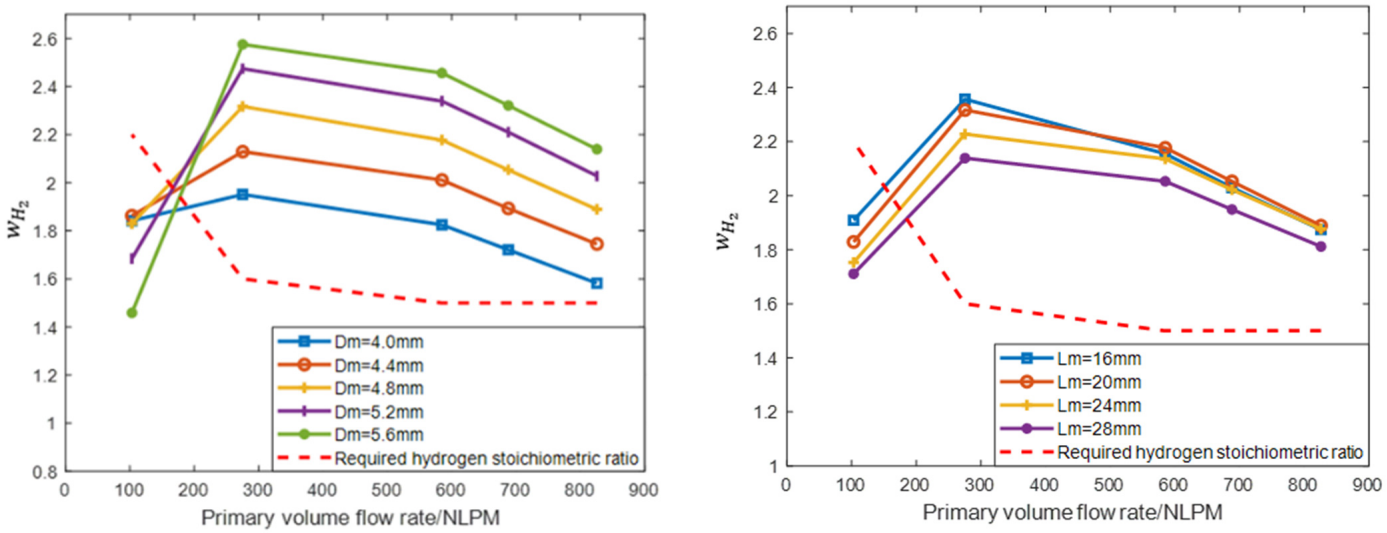

(**a**) (**b**)

Figure 6. Entrainment ratio at different geometric parameters: (**a**) hydrogen entrainment capability at various *Dm* with *Dn* = 1.32 mm; (**b**) hydrogen entrainment capability at different *Lm* with *Dn* = 1.32 mm, *Dm* = 4.8 mm, *NXP* = 3 mm.

Table 1. Optimized dual-ejector geometries.

	D_n (mm)	D_m (mm)	NXP (mm)	L_m (mm)	L_d (mm)	θ_d (°)
Ejector A	0.75	3	3	12	24	5
Ejector B	1.32	4.8	3	20	40	5

3.3. Ejector Test Results

A test bench for the dual-ejector system was built to evaluate each ejector's performance under different inlet and outlet pressures and various operation conditions. For safety reasons, pressurized air was used during the tests instead of hydrogen gas. The hydrogen supply and circulation system was designed for PEMFC hydrogen fuel gas flow. Simulations using the same boundary conditions and air to replace hydrogen gas were conducted to verify the CFD models using these air-based experiments. An air pump that could provide as high as 10 bara pressure was adopted to supply the high-pressure ejector primary inlet flow. A pressure and mass flow rate controller (PMC) was used before the two proportional valves (PV A and PV B) to adjust the required mass flow rate or pressure. In contrast, the integrated pressure and temperature sensors were applied to measure the pressure at the ejector inlet and outlets. Figure 7a shows that the test bench was only applicable for testing the pressure fluctuation at the ejector outlet. For the ejector performance test bench, the pipe between the buffer tank and the water separator and another connecting the water separator with the ejectors' secondary inlets were disconnected. In addition, two more proportional valves (PV C and PV D) were installed at points C and D to control the pressure of the ejector outlet and secondary inlet, respectively. Moreover, two more PMCs were applied before PV C and PV D to measure the mass flow rate at the secondary inlet and outlet.

Following the definition given in previous sections and Figure 4, Ports 1, 2, and 3 were for ejectors' primary inlet, outlet, and secondary inlet stream. The key parameters to be measured included the three mass flow rates of the ejector (m_1, m_2, and m_3) under controlled pressures (P_1, P_2, and P_3) of each port. The measured m_1, m_3 and calculated air entrainment ratio, as well as their comparisons to the CFD simulation results, are demonstrated in Figure 7b,c.

The CFD simulation results obtained from ANSYS Fluent used the same boundary conditions as the tests. The CFD predicted mass flow rates, and the experimentally measured mass flow rates of the two ejectors showed similar trends with different levels of errors. As shown on the right side of Figure 7b, the REs of the primary flow rate m_1 of ejector B between the CFD simulation and test results were below 8%. The larger ejector was easier to manufacture, and the nozzle of Ejector B was within the targeted diameter of 1.32 mm. As shown on the left side of Figure 7b, the REs of the m_1 of ejector A at low primary pressure P_1 under 5 bara were larger than 10%, while those at high P_1 were under 10%. The fine dimensions of the smaller ejector were challenging to control in manufacturing, leading to a noticeable deviation in the m_1 of Ejector A. Nevertheless, these errors were acceptable, since we were primarily concerned with the entrainment capability of the two ejectors, rather than their mass flow rates. Figure 7c shows excellent entrainment capabilities with entrainment ratios higher than 2 over an extensive range of variable flow rates for both Ejectors A and B. Here, the mean absolute percentage error (MAPE) was adopted to compare the test and simulation results: $MAPE = \frac{1}{n}\sum_{i=1}^{n}\frac{|y_i-\hat{y}_i|}{y_i} \times 100\%$, where y_i is the test result and $\hat{y}_i$ is the CFD simulation result at point i. The MAPE of the air entrainment ratio ω was 16.66% for Ejector B and 3.27% for Ejector A.

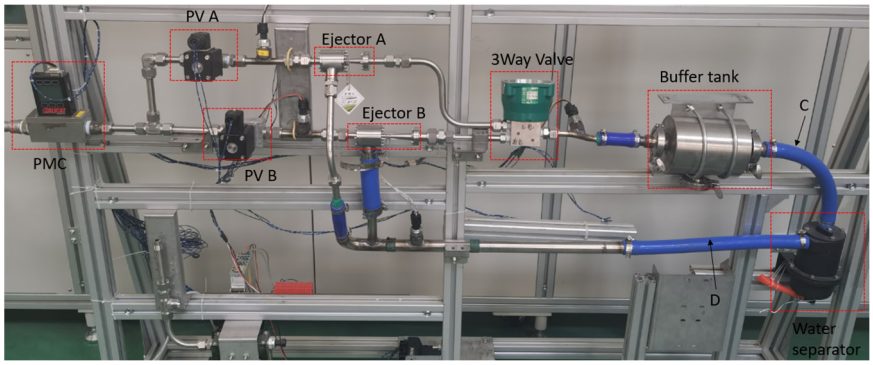

(**a**)

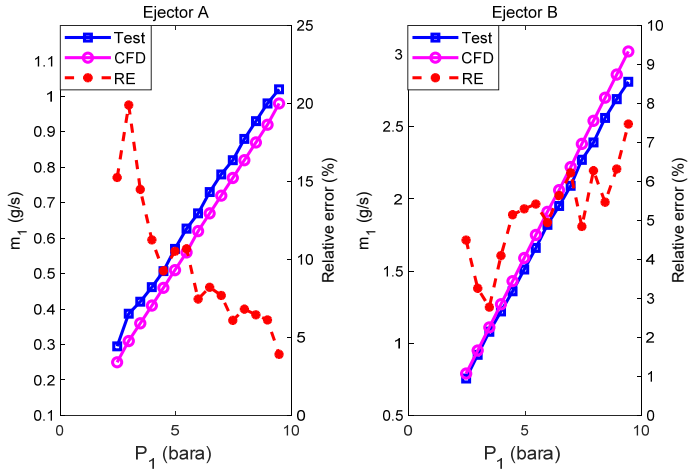

(**b**)

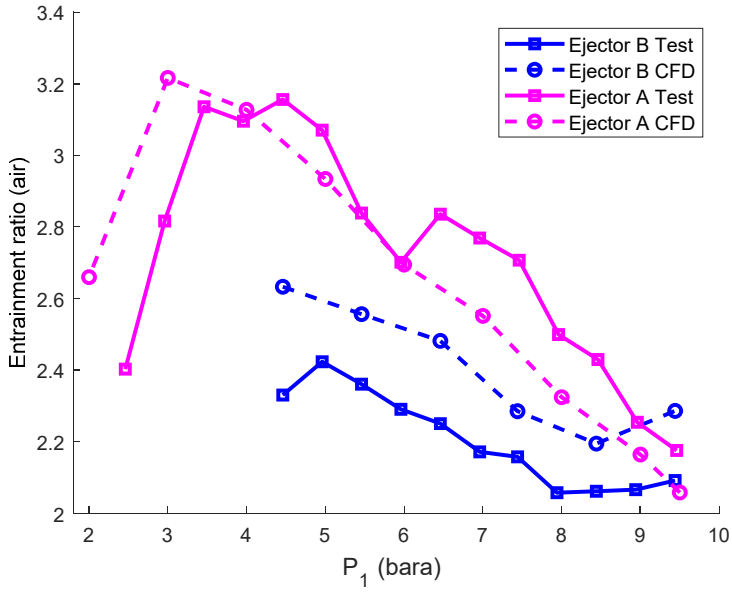

(**c**)

Figure 7. Comparisons of test and CFD simulation results. (**a**) Photograph of the test bench; (**b**,**c**) primary pressure P_1, mass flow rate m_1, relative error (RE), and entrainment ratio for Ejector A and Ejector B, respectively.

4. Optimal Control and Test of Dual-Ejector System

The control of ejectors with fixed dimensions relies on the accurate pressure and flow-rate adjustment of the primary inlet flow through proportional valves. Meanwhile, the secondary and outlet flows are connected to the fuel cell anode outlet and inlet. For this reason, the control of the hydrogen proportional valve is significant in achieving the best performance of the ejector. In the dual-ejector hydrogen supply and circulation system, each ejector has a proportional control valve with an electric actuator that can flexibly control the primary flow stream. In addition, a three-way valve can switch the gas flow path from either one of the dual-ejector to the fuel cell stack based on control policies.

The optimal operation control of the designed dual-ejector hydrogen system aimed at continuously supplying and effectively circulating fuel gas to the fuel cell stack for requested power at any time ($P_{req,t(i)}$). The smaller ejector (Ejector A) was activated during the lower power output from the stack. In contrast, the larger one (Ejector B) was responsible for the higher stack power. It was critical to identify the appropriate switching power (P_{switch}) at which the three-way valve was activated to shift gas flow from one to another. Depending on stack power output, the optimized operation control was conducted as shown in Figure 8.

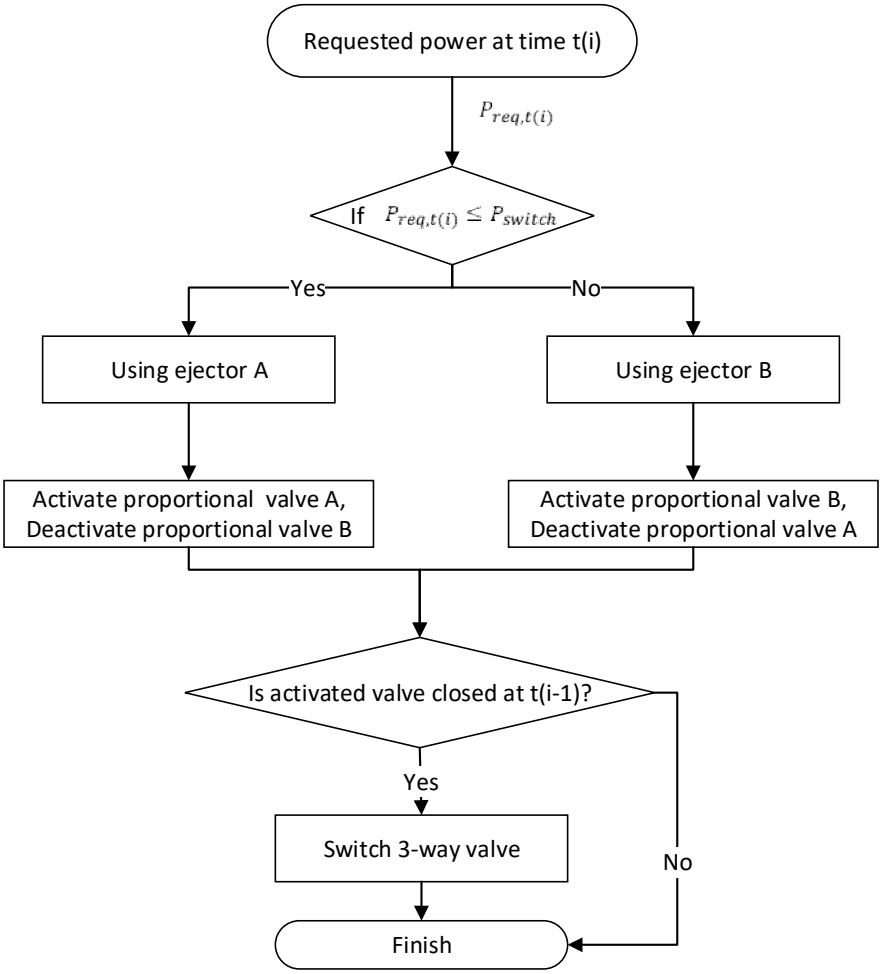

Figure 8. Control logic for the dual-ejector system.

4.1. Dual-Ejector System Analysis and Discussion

The test results of the designed dual-ejector system demonstrated an effective gas recirculation during a wide range of gas flow rates, covering the PEMFC operating from 40 A to 600 A. Specifically, Ejector A could cover the PEMFC stack operation from 6 kW to 27 kW, and Ejector B could cover it from 27 kW to 70 kW. Due to the limitation of the air

compressor's maximum inlet pressure on the test bench, the ejector performance above 10 bara of primary inlet pressure was not verified. The designed dual-ejector system was optimized to fully cover the PEMFC operation from 8% to 100% of stack power. Based on the test results, which only covered up to 55 kW, the remaining range from 55 to 70 kW can be anticipated to have good consistency with the CFD simulation.

The gas, when changing from air to hydrogen, can affect the entrainment ratio of ejectors. The CFD simulations using hydrogen gas for Ejectors A and B are shown in Figure 9. Both ejectors showed a higher entrainment ratio when hydrogen was used instead of air. Even when considering the MAPE of the air entrainment ratio, the hydrogen entrainment capability (ω_{H_2}) of both ejectors satisfied the stack hydrogen stoichiometric ratio requirement.

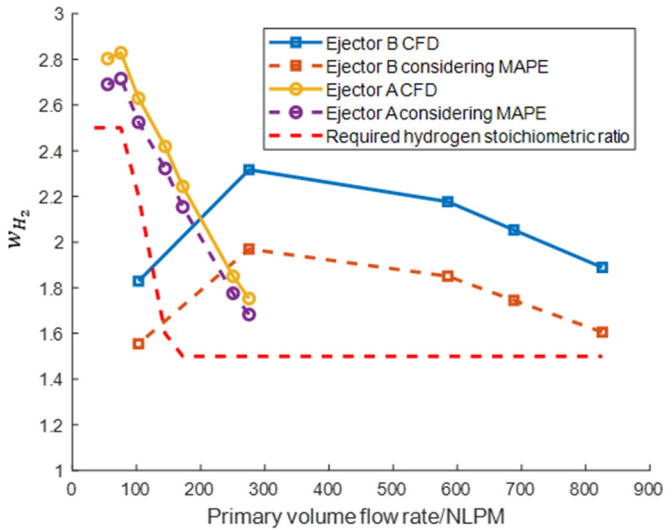

Figure 9. Hydrogen entrainment ratio achieved by the dual-ejector system under required stoichiometric ratio.

In Figure 9, the yellow line and blue lines indicate the CFD simulation of Ejectors A and B, respectively, using hydrogen. A high entrainment capability could be effectively achieved to fulfill the requirement of a hydrogen stoichiometric ratio from 8% to 100% of the PEMFC anode inlet gas (shown by the red dashed line). However, the entrainment capabilities of Ejectors A and B were slightly decreased, as shown by the red and purple dashed lines, when considering the MAPE generated from the simulation and test results using air. Nevertheless, both ejectors could still provide a high enough hydrogen stoichiometry to the system.

4.2. Discussion of Pressure Disturbances Using Dual Ejectors

The pressure fluctuation influenced by the transit process of changing hydrogen paths in a dual-ejector system is a primary concern. As required, the stack's hydrogen inlet pressure should be maintained stable, and the pressure differences between the anode and cathode should be adequately controlled. Drastic pressure fluctuation of hydrogen inlet may cause accumulated damage to the membrane and degrade its performance. Compared to a single-ejector system, a dual-ejector system has two different gas paths, and each path is equipped with an ejector suitable for a specific range of stack power output. In this work, Ejector A was optimally designed for the PEMFC's lower-power output, while Ejector B was for the high-power output. When the PEMFC output power exceeded the capacity of Ejector A, the hydrogen injection and circulation paths were shifted to the flow paths associated with Ejector B.

The three-way control valve in the system switched the gas circulation path between Ejector A and Ejector B back and forth, depending on the dual-ejector system's operation

control strategies. The different sizes of the flow chambers led to flow-rate variation during the switching process. As a result, pressure disturbances occurred due to the variant gas pressure and volume between the two paths.

As mentioned previously, using one proportional valve (shown in Figure 2a) could successfully control the primary inlet pressure and mass flow rate for both ejectors, since there was only one ejector at work each time the injection valve served. The dual-ejector system's three-way valve selected the stack's hydrogen-feeding path. When the gas path was switched from Ejector A to Ejector B, the proportional valve had to reduce pressure while maintaining the same mass flow rate. Therefore, the proportional and three-way valves were actuated simultaneously; the pressure and mass flow rate of the three ports were measured and plotted in Figure 10. We focused on the maximum absolute pressure variance of the discharged gas from the dual-ejector system ($max.|\Delta P_2|$) and the primary inlet pressure (P_1) response time $t(s)$ after switching the ejector. The $max.|\Delta P_2|$ was limited to a specific value to reduce the pressure impact on the PEMFC membrane. In addition, the system response time of P_1 had to be as fast as possible.

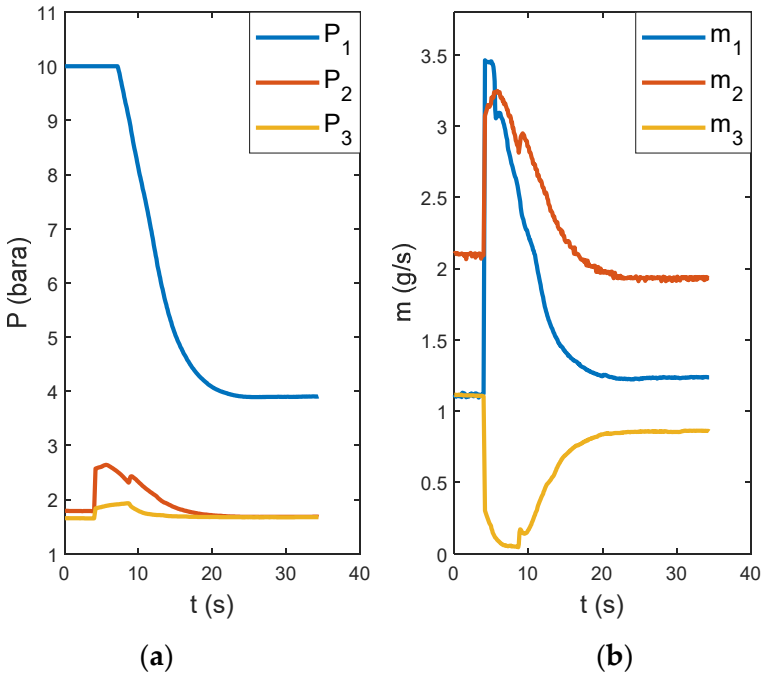

Figure 10. Pressure and mass flow rate fluctuation when switching from Ejector A to B: (**a**) pressure variation; (**b**) air mass flow-rate variation.

The ejector's primary inlet pressure was required to be reduced from 10 to 4 bara instantly while the three-way valve switched the gas path from the smaller Ejector A to the larger Ejector B. Meanwhile, the stack inlet mass flow rate had to be kept the same to maintain the hydrogen flow rate for the stack. The sudden change in gas paths induced a surge in the mass flow rate at the dual-ejector outlet and caused the pressure fluctuation of the discharged gas. The maximum difference in the outlet pressure $|\Delta P_2|$ with a simple switch was an unacceptable 94.8 kPa, as shown in Figure 10a. The response time of the primary inlet pressure change (P_1) was also very slow with only one proportional valve controlling the inlet pressure. By shifting the gas pathways, the sudden overflow of gas caused an increment in the mass flow rate in Path B, which induced the increased discharge mass flow (m_2) that cause the rise in pressure (P_2). Due to the increased pressure drop between the second inlet and outlet, the ejector entrainment capacity was decreased, as indicated by the reduced secondary inlet mass m_3.

To better understand and control the dynamic ejector-switching process, a system dynamics model was introduced to reflect the dynamic behavior of the system pressure

variation and identify the switching process's ideal operation parameters. A second-order system dynamic model was built in MATLAB/Simulink, and the transfer function was produced using experimental data of the switching process:

$$m\ddot{x} + c\dot{x} + kx = f(t) \tag{6}$$

where m, c, and k are constants identified using the system dynamic response experimental data.

For this system, the natural frequency $\omega_n = \sqrt{k/m}$ and the damping ratio $\zeta = \frac{c\omega_n}{2k}$ could also be obtained. Therefore, the transfer function can be written as:

$$H(s) = \frac{\omega_n^2}{s^2 + 2\zeta\omega_n s + \omega_n^2} = \frac{4}{s^2 + 4s + 4} \tag{7}$$

The objective of optimal operation control in the dual-ejector system was to maintain a constant pressure at the anode inlet (i.e., the pressure of the ejector's discharged port (P_2)) during the back-and-forth shifting of the gas path from Ejector A to Ejector B. A smooth increase and decrease in the total flow mass in the chamber during the switching process was vital to achieving this goal. However, the difference in chamber volume inherently caused sharp pressure disturbances, as illustrated in Figure 10. Therefore, optimal operation control during ejector switching was needed to address the issue.

The control variables for the dual-ejector system were the PWM control signals of the mass/pressure control valves that adjusted the ejector primary inlet conditions. When the dual-ejector hydrogen supply and circulation system used only one proportional valve, the operation control was accomplished by adjusting the timing of the pressure change. Using two proportional valves in the dual-ejector hydrogen supply and circulation system (Figure 2b), one for each path, could reduce the system pressure fluctuation more effectively. The two proportional valves opened and closed following different and coordinated rates during the switching process to ensure the total mass of the gas in the chamber remained almost constant, eliminating pressure variation. Moreover, more dynamic and accurate control could significantly reduce the system's response time.

This optimal switching process control problem can be formulated as:

$$\min_x f = [\Delta P_2,\ \tau]' x \in [x_{lb}, x_{ub}] \tag{8}$$

where x is the control variable (i.e., the PWM valve signals to adjust the proportional valve's pressure and mass); x is limited to the lower and upper boundary conditions (x_{lb} and x_{ub}); and f is the objective function, which was to minimize the pressure disturbance (ΔP_2) and the system's response time (τ).

Based on the dynamic model, a PID controller was added to the system to elicit a quick response to pressure changes. The ejector's primary inlet pressure responded faster to the PID controller, as shown in Figure 11.

With each ejector controlled by an individual gas-injecting valve, the pressure and mass flow rate were adjusted using PWM control signals. In this work, we compared the maximum pressure fluctuation (ΔP_2) caused by shifting the ejectors using only one inlet proportional valve (Figure 2a) vs. using two inlet proportional valves (Figure 2b). The results were tested and plotted below. The resulting pressure variations and response times were measured experimentally, as shown in Figure 12.

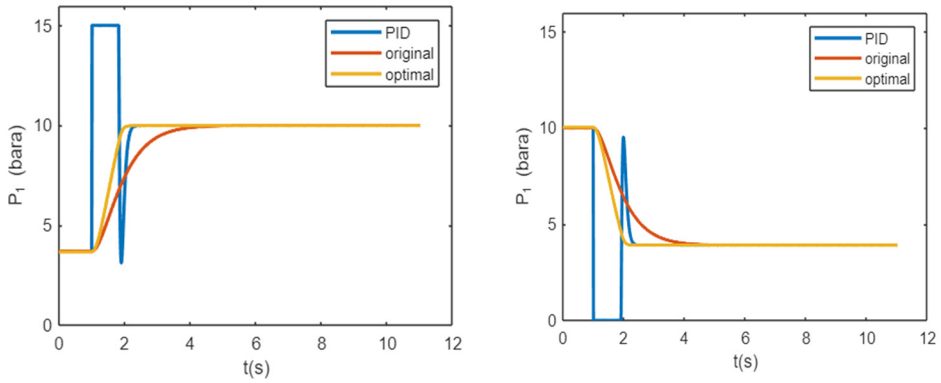

Figure 11. Dynamic pressure response of ejector's primary inlet with or without PID controller: (**a**) Switching from Ejector A to Ejector B; (**b**) switching from Ejector B to Ejector A.

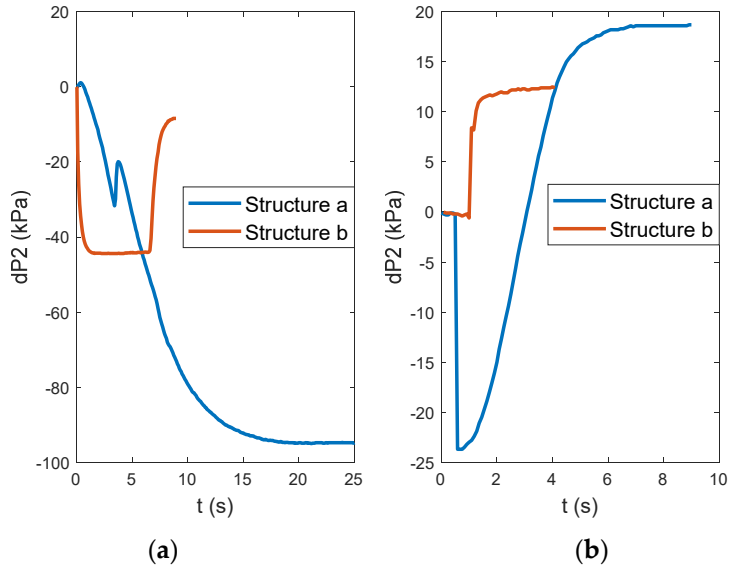

Figure 12. Pressure fluctuation during the transit-switching process of the dual-ejector system: (**a**) pressure fluctuation when switching from Ejector A to Ejector B; (**b**) pressure fluctuation during switching from Ejector B to Ejector A.

Figure 12a shows the measured stack inlet pressure fluctuation when switching from the small ejector to the large ejector, controlling one inlet proportional valve and two inlet proportional valves. With optimal control and using two proportional valves, the system response time was reduced from 13 s to 0.25 s, and the pressure fluctuation was significantly reduced from 95 kPa to 44 kPa. Figure 10b shows the measured pressure fluctuation when switching from the large ejector to the smaller one. Again, using two proportional valves could reduce the pressure fluctuation from a maximum of 24 kPa to 12 kPa and the response time from 3 s to 0.15 s.

The measured pressure disturbance and the predicted distribution from the Simulink models during the ejector switching were consistent, proving that the developed optimal control strategies for the proportional valves' operation could effectively minimize the anode side pressure disturbance. By reducing the dual-ejector hydrogen supply and circulation system's pressure variation, the impact on the PEMFC operational life was greatly reduced.

5. Conclusions

This research introduced a method for optimally designing and controlling the dual-ejector-based hydrogen fuel supply and circulation system of a PEMFC system. CFD modeling and simulations were applied in the design and control optimizations, and experimental tests were used to validate the simulation results and the newly introduced method. This paper demonstrated the full power output range covering the capability of the hydrogen supply and recirculation system using two ejectors for a 70 kW PEMFC stack with an improved net output power of the system. Specifically, a dual-ejector system paired with two hydrogen proportional valves was optimally designed and controlled to fully cover a PEMFC stack's operation from 40 A (or 6 kW) to 600 A (or 70 kW). The CFD simulations and bench test results of the optimally designed ejectors showed consistent and satisfactory entrainment ratios. Based on the testing results, the optimal controlled dual-ejector system could satisfy the required stoichiometric ratio of the hydrogen fuel in the entire operating range of the PEMFC system. Moreover, the optimal control strategies reduced the pressure fluctuations during the ejector switching to avoid potential harm to the PEMFC's operational life.

Author Contributions: Conceptualization, Z.D. and L.C.; methodology, L.C. and K.X.; software, K.X. and L.C.; validation, Z.Y. (Zuyong Yang) and Z.Y. (Zhen Yan); formal analysis, L.C. and K.X.; resources, Z.Y. (Zuyong Yang) and Z.Y. (Zhen Yan); writing—original draft preparation, L.C. and K.X.; writing—review and editing, Z.D.; visualization, K.X.; supervision, Z.D. All authors have read and agreed to the published version of the manuscript.

Funding: This research received no external funding.

Data Availability Statement: Not applicable.

Conflicts of Interest: The authors declare no conflict of interest.

References

1. Nikiforow, K.; Koski, P.; Ihonen, J. Discrete ejector control solution design, characterization, and verification in a 5 kW PEMFC system. *Int. J. Hydrogen Energy* **2017**, *42*, 16760–16772. [CrossRef]
2. Yumiya, H.; Kizaki, M.; Asai, H. Toyota fuel cell system (TFCS). *World Electr. Veh. J.* **2015**, *7*, 85–92. [CrossRef]
3. Eames, I.; Aphornratana, S.; Haider, H. A theoretical and experimental study of a small-scale steam jet refrigerator. *Int. J. Refrig.* **1995**, *18*, 378–386. [CrossRef]
4. Yin, Y.; Fan, M.; Jiao, K.; Du, Q.; Qin, Y. Numerical investigation of an ejector for anode recirculation in proton exchange membrane fuel cell system. *Energy Convers. Manag.* **2016**, *126*, 1106–1117. [CrossRef]
5. Fukuda, T.; Fukuma, K. Fuel Cell System and Method for Controlling Fuel Cell System. U.S. Patent Application No. US9356302B2, 31 May 2016.
6. Tanaka, S.; Nagumo, K.; Yamamoto, M.; Chiba, H.; Yoshida, K.; Okano, R. Fuel cell system for Honda CLARITY fuel cell. *eTransportation* **2020**, *3*, 100046. [CrossRef]
7. Jung, S.K.; Noh, Y.G.; Jeon, U.S. A development of the fuel cell system that the jet-pump is applied. In Proceedings of the ASME 2013 11th International Conference on Fuel Cell Science, Engineering and Technology, Minneapolis, MN, USA, 14–19 July 2013; American Society of Mechanical Engineers: New York, NY, USA, 2013.
8. Hosseinzadeh, E.; Rokni, M.; Jabbari, M.; Mortensen, H. Numerical analysis of transport phenomena for designing of ejector in PEM forklift system. *Int. J. Hydrogen Energy* **2014**, *39*, 6664–6674. [CrossRef]
9. Nikiforow, K.; Koski, P.; Karimäki, H.; Ihonen, J.; Alopaeus, V. Designing a hydrogen gas ejector for 5 kW stationary PEMFC system–CFD-modeling and experimental validation. *Int. J. Hydrogen Energy* **2016**, *41*, 14952–14970. [CrossRef]
10. Brunner, D.A.; Marcks, S.; Bajpai, M.; Prasad, A.K.; Advani, S.G. Design and characterization of an electronically controlled variable flow rate ejector for fuel cell applications. *Int. J. Hydrogen Energy* **2012**, *37*, 4457–4466. [CrossRef]
11. Sugawara, T.; Kizaki, S.; Nuiya, Y. Variable Flow-Rate Ejector and Fuel Cell System Having the Same. U.S. Patent Application US6858340B2, 22 February 2005.
12. Kim, M.; Lee, W.-Y.; Kim, C.-S. Development of the Variable Multi-ejector for a Mini-bus PEMFC System. *ECS Trans.* **2007**, *5*, 773–780. [CrossRef]
13. He, J.; Ahn, J.; Choe, S.-Y. Analysis and control of a fuel delivery system considering a two-phase anode model of the polymer electrolyte membrane fuel cell stack. *J. Power Sources* **2011**, *196*, 4655–4670. [CrossRef]
14. Liu, Y.; Tu, Z.; Chan, S.H. Performance enhancement in a H_2/O_2 PEMFC with dual-ejector recirculation. *Int. J. Hydrogen Energy* **2022**, *47*, 12698–12710. [CrossRef]

15. Fukuma, K.; Inoue, S. Ejector and Fuel Cell System Using the Same. European Patent Application US8329354B2, 11 December 2012.
16. Huang, B.; Chang, J.; Wang, C.; Petrenko, V. A 1-D analysis of ejector performance. *Int. J. Refrig.* **1999**, *22*, 354–364. [CrossRef]
17. Maghsoodi, A.; Afshari, E.; Ahmadikia, H. Optimization of geometric parameters for design a high-performance ejector in the proton exchange membrane fuel cell system using artificial neural network and genetic algorithm. *Appl. Therm. Eng.* **2014**, *71*, 410–418. [CrossRef]
18. Pei, P.; Ren, P.; Li, Y.; Wu, Z.; Chen, D.; Huang, S.; Jia, X. Numerical studies on wide-operating-range ejector based on anodic pressure drop characteristics in proton exchange membrane fuel cell system. *Appl. Energy* **2019**, *235*, 729–738. [CrossRef]